



**AN EMPIRICAL VALIDATION OF BUILDING SIMULATION SOFTWARE FOR
MODELLING OF DOUBLE-SKIN FACADE (DSF)**

Olena Kalyanova¹, Per Heiselberg¹, Clemens Felsmann², Harris Poirazis^{3,4}, Paul Strachan⁵, Aad Wijsman⁶

¹Department of Civil Engineering, Aalborg University, Aalborg, Denmark

²Technical University of Dresden, Dresden, Germany

³Department of Architecture and Built Environment, Lund Institute of Technology, Sweden

⁴Arup, United Kingdom

⁵Dept. of Mechanical Engineering, University of Strathclyde, Glasgow, Scotland, UK

⁶VABI Software BV, Delft, the Netherlands

ABSTRACT

Double-skin facade (DSF) buildings are being built as an attractive, innovative and energy efficient solution. Nowadays, several design tools are used for assessment of thermal and energy performance of DSF buildings. Existing design tools are well-suited for performance assessment of conventional buildings, but their accuracy might be limited in cases with DSFs because of the complexity of the heat and mass transfer processes within the DSF.

To address this problem, an empirical validation of building models with DSF, performed with various building simulation tools (ESP-r, IDA ICE 3.0, VA114, TRNSYS-TUD and BSim) was carried out in the framework of IEA SHC Task 34 /ECBCS Annex 43 “Testing and Validation of Building Energy Simulation Tools”.

The experimental data for the validation was gathered in a full-scale outdoor test facility. The empirical data sets comprise the key-functioning modes of DSF: 1. Thermal buffer mode (closed DSF cavity) and 2. External air curtain mode (naturally ventilated DSF cavity with the top and bottom openings open to outdoors).

By carrying out the empirical tests, it was concluded that all models experience difficulties in predictions during the peak solar loads. None of the models was consistent enough when comparing simulation results with experimental data for the ventilated cavity. However, some models showed reasonable agreement with the experimental results for the thermal buffer mode.

INTRODUCTION

Compared to a conventional fully glazed facade, a double skin façade (DSF) is multi-functional: it can function as a barrier for solar radiation, it can preheat the ventilation air, it can reduce the penetration of noise from the outside (e.g. traffic), it can allow secure application of night cooling, it can allow opening of windows in high storey buildings, etc. (Gertis, 1999).

Many studies have been performed worldwide to evaluate energy efficiency and thermal performance

of buildings with double facades. However, the results of these investigations show considerable variation: the calculated energy efficiency of DSFs varies between significant annual energy savings and major annual increases in energy use for cooling.

The design, dimensioning and application of DSFs is particularly important, because poor design can lead to increased energy use (mainly for cooling) and inferior indoor climate, compared to a building with conventional façade. Although there have been many validation studies that have helped to increase confidence in the use of existing design tools for the performance assessment of conventional buildings, their accuracy for prediction of double façade performance has not been tested to the same extent. To be able to design DSF buildings, engineers and architects must have confidence in simulation models for evaluating their thermal and energy performance.

To investigate the applicability of various thermal building simulation tools for modelling DSFs, an empirical validation of building simulation software was conducted in the frame of IEA SHC Task 34 /ECBCS Annex 43 “Testing and Validation of Building Energy Simulation Tools”. The main outcomes of this work are presented in this paper.

*Table 1
Organisations and programs participating in
empirical validation exercises*

Organization		Program
VABI	VABI Software BV Delft, The Netherlands	VA114
ESRU	Dept. of Mechanical Engineering University of Strathclyde Glasgow, Scotland	ESP-r
TUD	Technical University of Dresden Germany	TRNSYS- TUD
LTH	Division of Energy and Building Design Department of Architecture and Built Environment Lund Institute of Technology, Sweden	IDA ICE 3.0
AAU	Dept. of Civil Engineering Aalborg University, Denmark	BSim

Results of the empirical exercises are compared between several building energy simulation programs

and experiments. Table 1 includes a list of organizations who participated in the exercises and the simulation programs they used to perform the simulations. Simulations were carried out using IDA ICE 3.0; however, results obtained from this software are not included in the paper.

EMPIRICAL WORK

The empirical validation with experimental data gathered in autumn 2006 in the full-scale outdoor test facility ('The Cube', Figure 1) at Aalborg University.

'The Cube'

The 'Cube' consists of four domains: double-skin facade, experiment room, instrument room and plant room (Figure 2). The DSF in 'The Cube' is facing South and it has following internal dimensions: 3.5m width, 0.58m depth and 5.45m height.



Figure 1. Test facility, 'The Cube'.

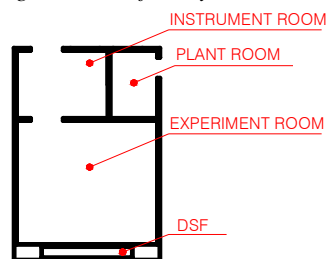


Figure 2. Plan of 'The Cube'.

The temperature in the experiment room was kept constant at approximately 22°C, using a ventilation system with the heating and cooling unit installed in the experiment room. In order to avoid temperature gradients in the experiment room, a recirculating piston flow with an air speed of approximately 0.2 m/s is used. This resulted in typical temperature gradient of approximately 0.02°C/m and maximum of 0.1°C/m. The air intake for recirculation is at the top of the room. After the intake the air passes through the preconditioning units of the ventilation system and then exhausted at the bottom of the room through fabric KE-low impulse ducts. Maximum power on cooling and heating units is 10 kW and 2 kW respectively. The transmission losses of 'The Cube' were determined experimentally.

For reliable estimation of ground-reflected solar radiation, a large carpet was placed on the ground in front of the southern façade of 'The Cube' to achieve uniform reflection from the ground. The fabric of the carpet was chosen so that it does not change its

reflectance property when it is wet due to its permeability. Reflectance is approximately 0.1, close to the generally assumed ground reflectance.

Absorption, reflection and transmission properties of all surfaces in the DSF, experiment room and windows were tested and available as a function of the wavelength, in the wavelength interval 250-2500nm. External windows of the DSF are of clear glass and internal windows are from VELFAC, low emissivity 4-Ar16-4.

Boundary conditions

The boundary conditions for the experimental work include measurements of weather parameters necessary to assemble a weather data file for thermal building simulation. These include wind speed, wind direction, outdoor air temperature, relative humidity, global and diffuse solar radiation, and atmospheric pressure. Besides that, the wind profile for the local terrain is established from 1-year measurement of wind speed and direction at six different heights above the ground.

For solar radiation measurements, two pyranometers were placed horizontally on the roof of 'The Cube'. Besides the weather data, the ground temperature below the foundation in the experiment room is specified as a boundary condition, together with the air temperature in the neighbouring zones (instrument room and plant room).

The air tightness of the building was measured with a blower door test and specified in the empirical test case specification (Kalyanova and Heiselberg, 2007a) available to the modellers. The discharge coefficients of the openings were estimated experimentally in a wind tunnel. The pressure coefficients are found from the literature (Straw, 2000), where pressure coefficients were measured for a building of the same dimensions as 'The Cube'.

Measurements

The duration of experiments was approximately 14 days for each mode. The experimental results, as well as weather data, are available for 1-hour and 10-minutes time interval. Results of calculations were compared against experimental data. The following are the parameters available for the comparison:

Primary parameters:

- Solar radiation striking on the external surface of the DSF
- Air temperature in the DSF cavity
- Cooling/heating load to experimental room
- Mass flow rate in the DSF cavity

Secondary parameters:

- Surface temperature of the glazing
- Surface temperature of opaque constructions

For more information about the experimental set-up and measurement procedure, see Kalyanova and Heiselberg (2007b).

The air temperature in the DSF cavity was measured, avoiding the impact of direct solar radiation on the sensor. To ensure that, each temperature sensor was coated with silver to ensure high reflectance. In addition, each sensor was shielded with a silver coated tube and ventilated by a minifan to ensure that the sensor measures the air temperature. The air temperatures in the DSF cavity were measured at six heights in the centre line of the cavity. The measurements were carried out with a sampling frequency of 5Hz and averaged for every 10 minutes.

The air flow in the double-skin facade cavity was measured using two methods: the velocity profile and tracer gas methods.

Velocity profile method. This method requires a set of anemometers to measure a velocity profile in the opening. The resolution of the determined velocity profile depends on the number of anemometers installed. Velocity profiles are measured at six levels, with different positioning of anemometers at each level. In total, 34 hot-sphere anemometers were used in the experimental set-up (Figure 3). The measurement frequency of the hot-sphere anemometers is 10 Hz.



Figure 3. Example: positioning of anemometers in the DSF cavity at $h=5.15m$.

Tracer gas method. The measurements were completed with the constant injection method. In this method, the tracer gas is injected at a constant rate and then the concentration response is recorded (Etheridge and Sandberg, 1996).

Carbon dioxide (CO_2) is the tracer gas used during the whole period of experiments. Carbon dioxide was released in the lower part of the double skin facade cavity, above the bottom openings. Even distribution of the tracer gas along the DSF cavity was ensured by its injection through a perforated tube. Samples of diluted tracer gas were taken at 12 points at the top of the DSF cavity, but below the top openings. All samples were mixed and then the concentration of the diluted tracer gas was measured by a gas analyzer. Concentration of carbon dioxide in the outdoor (incoming) air is measured continuously.

Accuracy and uncertainty of experimental data

Assessment of measurement accuracy is crucial for empirical validation. Here only the uncertainties related to the experimental methods are discussed and the accuracy of the instruments is reported. Prior to the measurements, the accuracy of all measurement equipment was checked. All of the instruments and sensors were calibrated for the suitable measurement conditions to reduce measurement uncertainty. The measurement uncertainty is summarised in Table 2.

Table 2.
Measurement uncertainty of equipment used in the experimental set-up.

<i>Temperature</i>	
HELIOS datalogger	+/- 0.07 °C
HBM datalogger	+/- 0.14 °C
<i>Solar radiation</i>	
Diffuse on horizontal surface	+/- 10 %
Total on horizontal surface	+/- 2%
Total on vertical surface (DSF)	+/- 3%
<i>Wind speed</i>	
3D ultrasonic anemometers	+/- 1 %
2D anemometers	+/- 4%
<i>Wind direction</i>	
3D ultrasonic anemometers	+/- 3°
2D anemometers	+/- 3°
<i>Cooling/Heating Load</i>	
Supply and return water temperature	+/- 0.1°C
Water mass flow rate	+/- 0.1%
Wattmeter	+/- 0.1 %
<i>Air velocities</i>	
Hot sphere anemometers	+/- 0.05 m/s
<i>Concentration of CO_2</i>	
In the DSF (BINOS)	+/- 10 ppm
In the outdoor air (URAS)	+/- 10 ppm

In the experimental studies, there are four experimental methods deserving special attention for uncertainty considerations. These are:

1. Measurement of air temperature under direct solar radiation
2. Measurement of air velocity with the hot sphere anemometers under direct solar radiation
3. Tracer gas method with constant injection of CO_2 for assessment of the air change rate in the DSF cavity
4. Velocity profile method for assessment of the air change rate in the DSF cavity

All described measurement methods have sources of error and compared to laboratory conditions have relatively large uncertainties. Although all the air flow measurement methods are difficult to use under such dynamic air flow conditions, their results show reasonable agreement and can be used for experimental validation of numerical models of natural ventilation air flow. In this paper attention is paid only to application of the tracer gas and velocity profile methods used for estimation of natural air flow in a double façade cavity (see Kalyanova and Heiselberg (2007b) for further details).

Tracer gas method with constant injection of CO_2 . This method requires the minimum amount of measurements and equipment, but it is characterized with frequent difficulties to obtain uniform concentration of the tracer gas, disturbances from wind wash-out effects and the time delay of the signal caused by the time constant of the gas analyzer (Kalyanova et al., 2007b).

According to McWilliams (2002), tracer gas theory assumes that tracer gas concentration is constant throughout the measured zone. For the tracer gas method an error in determined air flow is expected in

the range of 5-10 %, which requires full mixing of the tracer gas and air in the DSF cavity.

In the tracer gas method, the main errors appear when the tracer gas is not well mixed with the entrance air, or when there are wind wash-out effects, reversed flow and/or recirculation flow. With wind washout or flow reversal the tracer gas is removed from the DSF cavity: in practice this is indicated by very high readings of the air flow rate.

The wind washout effect is explained as an additional flow pattern that occurs in the DSF cavity, taking place in the horizontal plane. The main cause for its appearance is differences of wind pressure generated at different points in the adjacent horizontal openings on the same surface.

Comparing the characteristics of the errors, it was noted that the appearance of reverse flow is periodical (with weak buoyant forces, where the pressure coefficient at the top of the DSF is greater than that at the bottom) and these periods are relatively easy to identify. The wind wash-out effect is a similar phenomenon to reverse flow, but its occurrence is more random and originates from the highly fluctuating wind.

It is not possible to quantify the impact of poor mixing. The flow regime in the DSF cavity is turbulent and highly fluctuating; therefore, good mixing of air and tracer gas was expected, except when disturbed by wind washouts or flow reversal, causing removal of tracer gas from the cavity.

Velocity profile method. The velocity profiles are measured only in the central section in the cavity. Accordingly, one of the significant limitations in this method is the assumption of equal flow conditions in all three sections of the DSF cavity, which is not necessarily true in practice.

This method is also sensitive to the number of velocity sensors and their location in the plane, as poor approximation of the velocity profile will result in inferior accuracy. For better estimation of the velocity profile, knowledge of the flow conditions and flow patterns is needed.

Another limitation related to this method is the boundary layer flow, which can result in overestimation of the air flow rate in the cavity, both on days with strong solar radiation or at night. Accordingly, in the periods when the boundary flow at the surfaces of the DSF cavity is relatively strong, overestimation of mass flow rate will take place.

Empirical test cases.

Experimental data sets were compiled for two functioning modes of double-skin façade (Figure 4). These are:

1. Test case DSF100_e, which corresponds to thermal buffer mode. In this mode, all openings of the DSF were closed. Heat losses from the room to the outside are decreased when room temperatures exceed outside temperature.

2. Test case DSF200_e, which corresponds to external air curtain mode. The external operable windows at the top and bottom of the cavity were open. Typically, air enters the DSF at the bottom of the cavity, rises as it is heated in the cavity, then is released to the external environment removing some of the solar heat gains in the DSF. The flow motion in the cavity was naturally driven.

VALIDATION PROCEDURE

Simulation modelling

When attempting to model the specified test cases, simulation programs need to include interaction of the various heat and mass transfer processes occurring in the DSF. The methods of modelling these processes and interactions can differ significantly between simulation programs.

Geometry. The geometry of the DSF in 'The Cube' is complex: there are 9 windows, containing a transparent part (glazing) and an opaque part (window frame). The modellers made their assumptions regarding simplification of the geometry: the areas of the window frame and glazing were kept according to the specification, but the geometry definition was changed.

The DSF cavity was modelled differently in the programs. In ESP-r, the cavity was modelled as three zones stacked on top of each other (for DSF200_e). In TRNSYS-TUD, the cavity was modelled as 4 zones, with two smaller zones located at the bottom and at the top and two bigger ones located in the middle of the cavity. In BSim and VA114, the cavity was modelled as one thermal zone.

Transmission of solar radiation. The software programs treat diffuse and direct solar radiation separately when calculating transmission and distribution of solar radiation; however, different calculation methods are used. In all of the programs except for TRNSYS-TUD the direct solar radiation was treated as direct after passing the first layer of fenestration (external layer) and after the second layer (internal layer). In the TRNSYS-TUD model the direct solar radiation is treated as diffuse when passing the second layer of fenestration.

Surface heat transfer. For both operational strategies of the DSF, the air temperature in the DSF cavity is a consequence of convective heat transfer between the heated surfaces of glass and air. The floor, ceiling and side walls of the DSF have little importance due to their relatively small areas.

Air (mass) flow models. Depending on outdoor conditions and double skin facade functioning mode the air flow rate in a ventilated cavity can have significant variation in order of magnitude and in occurrence of wind wash out effect or flow reversal. In contrast, in a mechanically or naturally ventilated room the minimum air change rate is specified in

requirements for the indoor air quality, while the maximum is normally restricted by energy savings considerations or comfort conditions. The variation of the flow magnitude may result in variation of the flow regimes and will further complicate the situation.

The pressure coefficients were specified for both the top and bottom openings of the DSF. These were used in the ESP-r and TRNSYS-TUD programs, while in VA114, due to the same orientation of the openings, ΔC_p is modelled as zero (Table 3). Here, it can be argued that for the openings on the same surface, the wind pressure component is fairly weak and the wind turbulence can become more significant. From all of the models only the VA114 model includes the impact of the wind turbulence on the magnitude of mass flow in the cavity. All programs use the network pressure model for

calculating natural ventilation flow rates in the cavity, except BSim which uses the experimental method (empirical relationships for the air flow rates depending on temperature, wind speed, pressure difference coefficients and the discharge coefficient). In BSim, the impact of wind pressure is included by application of another empirical coefficient.

Thermal bridge losses. These were quantified according to available experimental data of the heat losses in the test facility for two periods with overcast sky, calm wind conditions and relatively constant air temperature during 24 hours.

All models were adjusted identically to account for thermal bridge losses. Results of the adjustments are illustrated for a steady-state exercise in Figure 4, where the deviation between the programs and the experimental data was small (20W) compared to earlier results without adjustments (250W).

Table 3.
Comparison of air flow models used in the empirical models.

Software		BSim	VA114	ESP-r	TRNSYS-TUD
Influencing parameters in the flow model	wind force	x	x	x	x
	wind fluctuations	-	x	-	-
	buoyancy	x	x	x	x
Air flow model		experimental	network	network	network
Pressure-Air flow relationship used			power-law	orifice	power-law
Discharge coefficient		as in spec.0.65/0.72	0.61	as in spec. 0.65/0.72	0.65
Pressure difference coefficients		$\Delta c_p = 0$, but wind impact is included by application of c_r -coefficient	$\Delta C_p = 0$	as in spec	as in spec

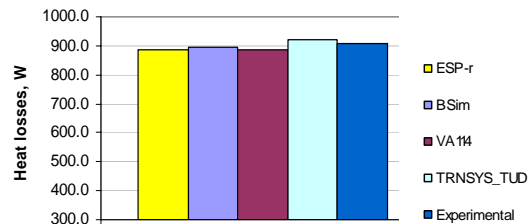


Figure 4. Total heat losses from the experiment room, modified to account for thermal bridges. (Kalyanova and Heiselberg, 2008).

Results of simulation

Surface heat transfer. Sensitivity to assumptions made of surface heat transfer models in the programs was investigated by sensitivity study. More details about the results of this study can be found in Kalyanova and Heiselberg (2008). Different (combined and split, fixed and variable) surface coefficients were applied in the VA114 and ESP-r models. It was concluded that the assumptions regarding the surface heat transfer in the model are crucial for simulation of buildings with double-skin facades. It is necessary to stress that the assumptions must be considered for two levels of detail when modelling surface heat transfer:

- Separate or combined treatment of surface film transfer
- Fixed or variable surface film coefficients

More attention is needed when modelling internal convective heat transfer and longwave radiation heat exchange. Deviations may appear in calculations for peak loads of solar radiation if using fixed combined surface film coefficients.

Boundary conditions. Glazing area of the double skin facade windows at the outer skin is 16.2 m², so differences in predictions of solar irradiation of $\pm 10 \text{ W/m}^2$ will result in $\pm 160 \text{ W}$ difference in incident solar radiation on the glazing surface. Good agreement between the programs was achieved when comparing their calculation of solar altitude. When calculating incident direct solar radiation striking the external surface of the DSF, the deviation of the mean values is nearly negligible, while the deviation of maximum values between the programs is about $\pm 10 \text{ W/m}^2$. Calculations of the diffuse solar radiation are also in agreement when the mean values are concerned. The maximum values show greater variation, probably due to high variation of cloud distribution in the sky. All programs agree well on calculation of incident total solar radiation on the external window surface when comparing the mean values. Comparing the maximum values the experimental data seems to be slightly lower and the disagreements are more pronounced (Figure 6).

The total solar irradiation on the vertical surface of the DSF was measured. Some measurement uncertainty is present due to frequent rain drops on

the pyranometer. This can contribute to the higher incident solar radiation according to the models compared to the experimental data.

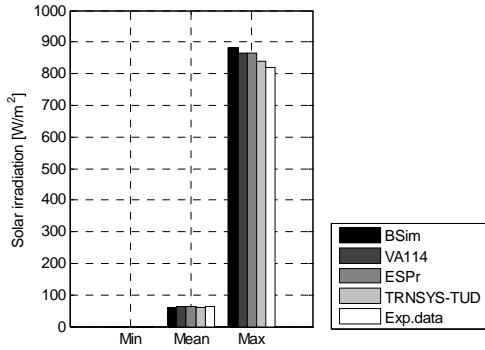


Figure 5. Total solar radiation on the external DSF surface. DSF100_e.

DSF100_e. In Figure 6, the air temperature in the cavity is shown for two days with different solar radiation intensity. All models fit well with the experiments on a cloudy day and have a spread of 10-15°C on a clear day. ESP-r agrees well with the dynamics of the air temperature measured in the cavity (it also has the lowest standard error), especially in the afternoons, while all of the other models show significant temperature drop.

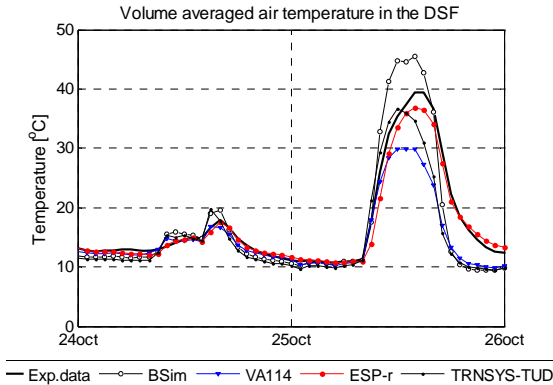


Figure 6. Volume averaged air temperature in the double facade cavity. DSF100_e.

Most of the programs underestimate the cooling power in the zone, especially during peak loads (Figure 8). It is characteristic that BSim predicts the highest cooling power, which is consistent with overestimation of the air temperature in the DSF cavity, and due to the fact that all solar radiation approaching the internal surfaces in the model is assumed to be fully absorbed. For the other models, underestimation of cooling loads is also consistent with underestimation of air temperature in the cavity.

Since the agreement between the measurements and simulations is poor only for the periods of peak loads, the performance of the programs for determining mean values is satisfactory. However, this is not enough when assessing the performance of the dynamic models.

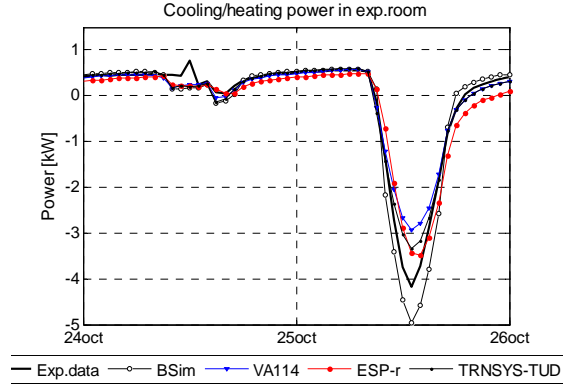


Figure 7. Cooling/heating power in the experiment room. DSF100_e.

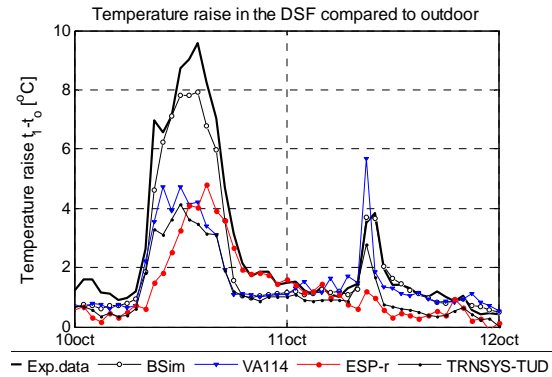


Figure 8. Temperature rise in the DSF cavity compared to the outdoor air temperature. DSF200_e.

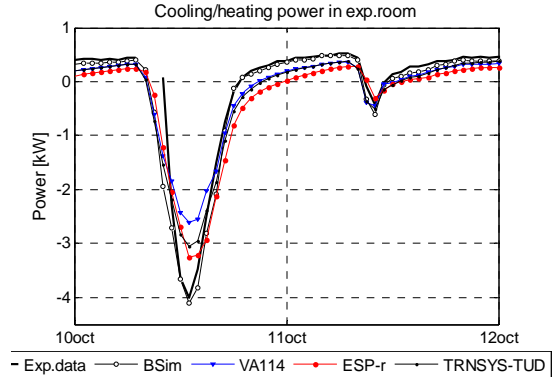


Figure 9. Cooling/heating power in the experiment room. DSF200_e.

DSF200_e. In view of fact that the air flow rate in a double skin facade cavity can be high, it is essential to perform the empirical validation of the air temperature predictions in the models using the temperature rise in the cavity compared to the outdoor air temperature (Figure 9). An error in prediction of cavity air temperature of 1°C can mean hundreds of watts of error in the energy balance of DSF.

All models underestimate the air temperature in the cavity. The absolute mean error varies between 0.5 and 1°C, corresponding to energy transport with the

mass flow of approximately 0.2-0.3 kW, when the mass flow is 1000 kg/h. Certainly, the accuracy of the measurements become even more important here, since the range of temperature variation is small.

Empirical validation of naturally induced mass flow rates in the DSF cavity is difficult because the flow is complex and difficult to measure accurately. The stochastic nature of wind (giving non-uniform, dynamic flow conditions), in combination with the assisting or opposing buoyancy force, cause the main difficulties.

Considering predictions of the natural air flow rate in the DSF cavity, it is not enough to consider a 2-day interval. In this paper, the results from the complete test period are included in Figure 10, where the results of predictions are compared against experimental data obtained with the tracer gas method, and in Figure 11, where the results are

compared against the velocity profile method. Evaluation of these results requires assessment of measurement errors and uncertainties of the experimental methods. In Figure 10 (tracer gas method), results of simulations and experimental results appear fluctuating and random for the first half of the period, while in the second half it is easy to distinguish between periods with high and low solar radiation. It is likely that the haphazard air flow rate in the DSF cavity during the first half period is caused by frequent variations in the wind directions between the south-east and south-west and high wind speeds above 6m/s. More stable wind direction, relatively calm wind conditions (below 6 m/s), cooler outdoor temperatures and less changeable solar radiation resulted in more consistent simulation results in the later parts of the experiment.

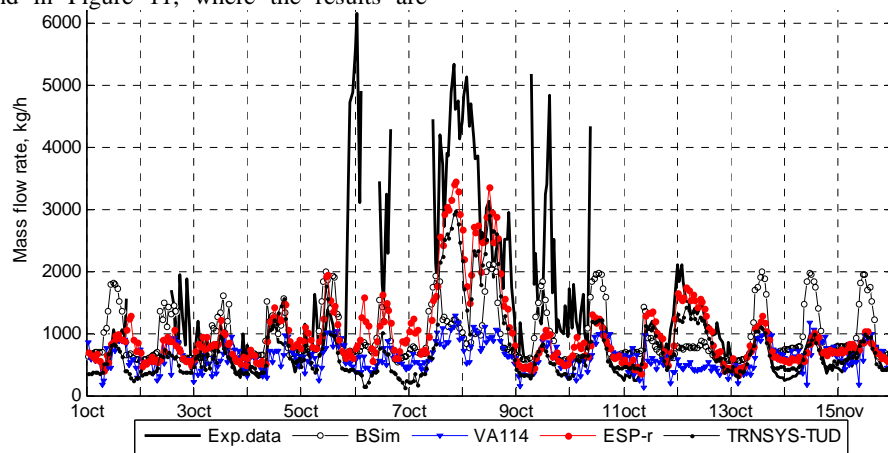


Figure 10. Hourly averaged mass flow rate in the DSF cavity, measured with the tracer gas method. DSF200_e.

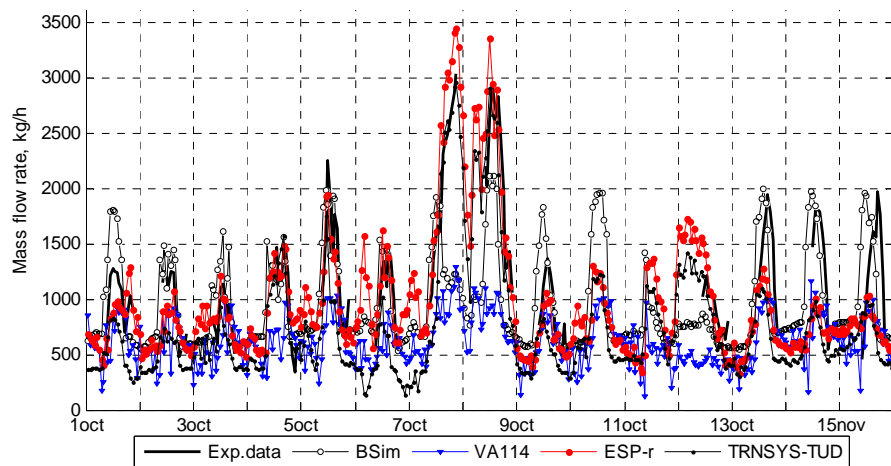


Figure 11. Hourly averaged mass flow rate in the DSF cavity, measured with the velocity profile method at $h=1.91m$. DSF200_e.

Night- and day-time periods are less clearly identified in the VA114 program. This is partly due to the model, which includes the impact of wind fluctuations on air flow rate in the cavity. Also, this model does not include direct influence of the wind forces, such as pressure difference at the openings.

The mass flow rate is calculated based on zone air temperature at the end of the previous time step, resulting in greater fluctuations in mass flow rate. BSim often overestimates the air flow rate, during both day and night time; however, in periods of high

wind speed, air flow rate is underestimated, caused by the simplified empirical air flow model.

For the velocity profile method (Figure 11) there is better agreement between experimental results and calculations, although the order of error is still in the range of 500 kg/h.

Simulation and measurement of naturally induced flow rates is difficult. Therefore, the similarities in the shapes between measurements and simulations for the TRNSYS-TUD and ESP-r programs are encouraging. Both these programs take into the consideration the individual pressure coefficients for each opening – this is important when modelling naturally induced flow. However, no preferences should be given to any particular method without consideration of experimental errors.

The evaluation of the results against the empirical data is difficult, as there are two sets of results available. The estimation of the accuracy of these two methods is still the weak point in the validation procedure. There is also a strong disagreement between the predictions by different programs.

DISCUSSION

The majority of validation studies have historically been undertaken with comparatively simple configurations. This paper has described a detailed empirical validation study of a highly complex domain.

With regard to the results from test case DSF100_e, despite limitations of the experimental data, some models appear to be consistent with the experimental results, except for modelling of peak solar loads.

The deviations between the measured and simulated cooling/heating power in the experiment room are large for test case DSF200_e. Most of the models underestimate the cooling loads to the zone especially in days with intensive solar irradiation, while at night, better agreement is reached. It is noteworthy that occasionally models have good agreement with the experimental data, but it is not consistent through the whole exercise.

Underestimated cooling power and thus underestimated heat flux through the interior skin of DSF can most likely be explained by:

- underestimation of DSF cavity air temperature
- errors in prediction of cavity mass flow rate
- underestimation of solar gains to DSF and/or experiment room
- limitations of the experimental set-up and errors in modelling the experiment room time constant

More detailed modelling of vertical temperature gradient in the DSF cavity can be achieved by splitting it into several thermal zones.

Improvement of the thermal model requires more knowledge of the convective and flow regimes in the cavity. A dynamic model for estimation of convective heat transfer in the DSF could be

beneficial for different modes of operation, as application of combined film coefficients appears to be inappropriate and application of fixed film coefficients does not prove to be satisfactory. However, it requires knowledge of which dynamic model is suitable for DSF cavities.

Air flow rate, flow regime, convective and radiative heat transfer have an impact on the resulting air temperature in the cavity. To be successfully validated a model has to demonstrate consistency of predictions for all parameters and have certain agreement with the experimental data. For the moment, none of the models appeared to be consistent enough when comparing results of simulations with the experimental data.

The disagreements between the models and experiments identifies a problem: further research is needed to solve these problems. The results of this empirical validation are regarded as an argument for further search for improvements, as most of the results do not allow deriving any solid conclusions, and only identify the research directions to follow.

ACKNOWLEDGEMENT

This work was conducted in the framework of IEA SHC Task 34 /ECBCS Annex 43 “Testing and Validation of Building Energy Simulation Tools” and was financially supported by the Danish Technical Research Council (Grant 2058-03-0100).

REFERENCES

- Etheridge D., Sandberg M. 1996. Building Ventilation: Theory and Measurement, John Wiley, Chicester.
- Gertis K. 1999. Sind neuere Fassadenentwicklungen bauphysikalisch sinnvoll? Teil 2: Glas-Doppelfassaden (GDF) (in German), Bauphysik, vol. 21, pp. 54-66.
- Kalyanova O., Heiselberg P. 2007a. Final Empirical Test Case Specification: Test Cases DSF100_e and DSF200_e. Aalborg University, Department of Civil Engineering. Technical Report No.33.
- Kalyanova O., Heiselberg P. 2007b. Experimental Set-up and Full-scale Measurements in ‘The Cube’. Aalborg University, Department of Civil Engineering. Technical Report No.34.
- Kalyanova O., Heiselberg P. 2008. Empirical Validation of Building Simulation Software: Modelling of Double Facades: Final Report. Aalborg University, Dept. of Civil Engineering.
- McWilliams J. 2002. Review of Airflow Measurement Techniques. Lawrence Berkeley National Laboratory.
- Straw M.P. 2000. Computation and Measurement of Wind Induced Ventilation: PhD thesis. Nottingham University.